RSC Advances

PAPER

View Article Online
View Journal | View Issue

Check for updates

Cite this: *RSC Adv.*, 2021, **11**, 15360

Guanidine functionalized core–shell structured magnetic cobalt-ferrite: an efficient nanocatalyst for sonochemical synthesis of spirooxindoles in water†

Mahla Dadaei and Hossein Naeimi *

Received 4th February 2021
Accepted 15th April 2021

DOI: 10.1039/d1ra00967b

rsc.li/rsc-advances

Core/shell nanoparticles have a wide range of applications in the science of chemistry and biomedicine. The core–shell material can be different and modified by changing the ingredients or the ratio of core to the shell. In this research, a $CoFe_2O_4$@SiO_2-guanidine nanocomposite was prepared and identified as an efficient catalyst for the one-pot synthesis of spirooxindole derivatives in water under ultrasonic irradiation conditions. The advantages of this method are in its simplicity, saving costs and energy, high yields, short reaction times, environmental friendliness, reusability and easy recovery of the catalyst using an external magnet. The catalyst was characterized by XRD, SEM, TEM, EDX, FT-IR, TGA and VSM techniques.

Open Access Article. Published on 10 May 2021. Downloaded on 1/20/2026 11:24:10 AM.
This article is licensed under a Creative Commons Attribution-NonCommercial 3.0 Unported Licence.

1. Introduction

Spirooxindole alkaloid compounds were first extracted from plants of the Apocynaceae and Rubiaceae families.[1] Synthesis of spiroxindole compounds among organic chemists is particularly important because these heterocyclic compounds have a wide range of pharmacological activities.[2] These spirocycles possess anticancer and antimicrobial activities.[3] They are also known to exhibit analgesic, anticonvulsant,[4] and fungicidal[5] activities.

Recently, few synthetic methods for the synthesis of spiroxindoles have been reported in the literature. Some of the catalysts that have been utilized in these methods are; PPh_3,[6] $HAuCl_4 \cdot 3H_2O$,[7] $InCl_3/SiO_2$,[8] sodium stearate,[9] and ethylenediamine diacetate (EDDA).[10]

However, there are disadvantages to these reported methods, such as; a poor yield, the use of toxic solvents, protracted reaction time and reusability of the catalyst is hardship. Although, each of the known methods for the synthesis of spirooxindole compounds has its competency, however further studies are still necessary for the efficient, environmental and economical multicomponent methodology for the synthesis of these heterocyclic compounds.

The use of ultrasonic waves in organic synthesis has been boosted in recent years.[11,12] This technique has many advantages including saving costs and energy, nontoxic, environmentally friendly solvent[13,14] and reduce of side products.[15] The power of ultrasound radiation is (20 kHz to 10 MHz).[16] Ultrasound irradiation could be positive effect on increasing yields and rate of the reaction due to the mechanical effect of shock waves. The main event in sonochemistry is the creation, growth and collapse of a bubble that is formed in the liquid. The step leading to the growth of the bubble occurs through the diffusion of solute vapor into the volume of the bubble. The last stage is the crash of the bubble, which occurs when the bubble size reaches its maximum value.

Core/shell nanoparticles have a wide range of applications in the science of chemistry, biomedical, pharmaceutical, electronics and catalysis. Therefore, these nanoparticles have attracted the attention of researchers. The core–shell material can be different and modified by changing the ingredients or the ratio of core to the shell.[17] Due to the coating of the shell material, the reactivity of core decreases and the thermal stability changes. The purpose of the core cover surface modification, reduce the consumption of precious metals and increase the efficiency of functional groups. In recent years, the applications of core–shell structured MNPs in organic reactions have developed.[18–24]

Herein, we would like to report the synthesis and application of guanidine immobilized on $CoFe_2O_4$@SiO_2-CPTES nanocomposites as an environmentally benign, highly efficient and reusable catalyst for the preparation of spirooxindole derivatives *via* one-pot three component of isatin or 5-chloroisatin, malononitrile or cyanoacetic esters and 1,3-dicarbonyl compounds in water under ultrasonic irradiation.

2. Experimental

2.1. General information

The chemicals were purchased from Fluka and Merck Chemical Companies and used without purification. ^{1}H NMR was recorded in DMSO-d_6 solvent on a Bruker DRX-400

Department of Organic Chemistry, Faculty of Chemistry, University of Kashan, Kashan, 87317, I. R. Iran. E-mail: naeimi@kashanu.ac.ir; Fax: +98 3615912397; Tel: +98 3615912388

† Electronic supplementary information (ESI) available. See DOI: 10.1039/d1ra00967b

© 2021 The Author(s). Published by the Royal Society of Chemistry

Open Access Article. Published on 10 May 2021. Downloaded on 1/20/2026 11:24:10 AM. This article is licensed under a Creative Commons Attribution-NonCommercial 3.0 Unported Licence.

spectrometer with tetramethylsilane as internal reference. FT-IR spectra were obtained as KBr pellets on a Perkin-Elmer 781 spectrophotometer and on an impact 400 Nicolet FT-IR spectrophotometer. The nanostructures were characterized using a Holland Philips Xpert X-ray powder diffraction (XRD) diffractometer (CuK, radiation, $k\frac{1}{4}0.154056$ nm), at a scanning speed of 2° min^{-1} from 100 to 100° (2Ø). The morphological study of the nanocomposites was investigated by scanning electron microscopy (SEM, SIGMA VP). The Electron Dispersive X-ray (EDX) analysis of the catalyst was performed on Oxford Instrument Company. The nanocomposite was investigated by transmission electron microscopy (TEM, Zeiss-EM10C-100 kV). Thermogravimetric analysis (TGA) was performed on a mettler TA4000 system TG-50 at a heating rate of 10 K min^{-1} under N_2 atmosphere. The magnetic properties of nanoparticles have been measured with a vibrating sample magnetometer (VSM, PPMS-9T) at 300 K in Iran (Kashan University). Melting points were obtained with a Yanagimoto micro melting point apparatus and are uncorrected. The purity determination of the substrates and reaction monitoring were accomplished by TLC on silica-gel polygram SILG/UV 254 plates (from Merck Company).

2.2. Catalyst preparation

2.2.1. General procedure for preparation of $CoFe_2O_4$ nanoparticles. Firstly, cobalt ferrite nanoparticles ($CoFe_2O_4$) were synthesized by co-precipitation procedure, according to the reported method in the literature.[25] The 3 g solution of sodium hydroxide was added drop wise to a mixture of $CoCl_2 \cdot 6H_2O$ (1.19 g) and $FeCl_3 \cdot 6H_2O$ (2.70 g). The pH of the solution was constantly monitored as the NaOH solution was slowly added. The reactants were stirred using a magnetic stirrer till the pH of the solution was close to 13 for 1 h at reflux temperature. The black precipitate of $CoFe_2O_4$ were centrifuged and washed several times with double distilled water and ethanol. The acquired substance was calcined for 4 h at 300 °C.

2.2.2. General procedure for preparation of nano-$CoFe_2O_4$@SiO_2 core–shell. The core–shell $CoFe_2O_4$@SiO_2 nanoparticles were obtained according to the reported method in the literature with minor modifications.[25] 1 g of the $CoFe_2O_4$ NPs was dispersed in 10 mL deionized water and 20 mL absolute ethanol by sonication for 30 min. Then, 5 mL NH_3 and 1 mL tetraethylorthosilicate (TEOS) were added to the reaction mixture and was stirred at 40 °C for 24 h under the condition of N_2 atmosphere. Finally, the precipitates, $CoFe_2O_4$@SiO_2 MNPs, were washed with deionized water and ethanol for 3 times and dried at 80 °C for 10 h.

2.2.3. Preparation of $CoFe_2O_4$@SiO_2-CPTES. The surface of silica nanoparticles can be easily functionalized and were obtained according to the reported method in the literature with minor modifications.[26] To 2.5 mL of the 3-chloropropyltriethoxysilane (CPTES) was slowly added 1 g of $CoFe_2O_4$@SiO_2 MNPs solution suspended in dry toluene. The solution was refluxed for 24 h under an inert atmosphere, filtered and washed subsequently with toluene, dichloromethane and dried at 80 °C for 10 h.

2.2.4. Preparation of $CoFe_2O_4$@SiO_2-guanidine. Finally, according to the reported method in the literature with modifications,[26] the amount of 1 g of $CoFe_2O_4$@SiO_2-CPTES was dispersed in 10 mL of toluene in an ultrasonic bath for 10 min. A mixture of functionalized MNPs was added to a suspension of Na_2CO_3 (0.34 g) and guanidine (0.56 mL). The mixture was refluxed for 30 h at 110 °C. The $CoFe_2O_4$@SiO_2-guanidine thus obtained, washed with double distilled water until neutrality, further washed with ethanol and dried at room temperature.

2.2.5. General procedure for the synthesis of spirooxindole derivatives. A mixture of isatin (1 mmol, 0.147 g) or 5-chloroisatin (1 mmol, 0.182 g), malononitrile (1 mmol, 0.07 g) or cyanoacetic ester (1 mmol, 0.102 mL), 1,3-dicarbonyl compounds in water and $CoFe_2O_4$@SiO_2-guanidine (8 mg) was added and reacted under ultrasonic irradiation (40 W). The progress of the reaction was monitored by thin layer chromatography (TLC) and was used ethyl acetate/petroleum ether (1/2) as an eluent. After completion of the reaction, the catalyst was separated by an external magnet. The organic residue was washed with water for several times and dried under vacuum to give the pure product. The products were confirmed by spectral data and physical data.

2-Amino-2′,5-dioxo-5H-spiro[indeno[1,2-b]pyran-4,3′-indoline]-3-carbonitrile. Yellow solid, mp 207–210 °C. IR (KBr) ν(cm^{-1}): 3316, 3193, 2201, 1731, 1669, 1602, 1470, 1336, 1212. ^{1}H NMR (400 MHz, DMSO-d_6) δ (ppm): 6.87 (d, 1H, Ar–H, J = 8.0 Hz), 6.95 (t, 1H, Ar–H, J = 8.0 Hz), 7.21 (d, 1H, Ar–H, J = 4.0 Hz), 7.24 (s, 1H, Ar–H), 7.29 (d, 1H, Ar–H, J = 4.0 Hz), 7.36 (d, 1H, Ar–H, J = 8.0 Hz), 7.43 (t, 1H, Ar–H, J = 8.0 Hz), 7.56 (t, 1H, Ar–H, J = 8.0 Hz), 7.70 (s, 2H, NH_2), 10.68 (s, 1H, NH). ^{13}C NMR (100 MHz, DMSO-d_6) δ (ppm): 45.69, 57.08, 107.17, 109.71, 117.34, 118.78, 122.17, 122.23, 124.57, 129.12, 130.43, 131.30, 131.98, 133.64, 135.07, 141.77, 160.41, 167.47, 177.34, 189.34.

7′-Amino-2,4′-dioxo-2′-thioxo-1′,2′,3′,4′-tetrahydrospiro [indoline-3,5′-pyrano[2,3-d]pyrimidine]-6′-carbonitrile. White solid, mp 232–235 °C, lit. [27] (mp 240–241 °C). IR (KBr) ν(cm^{-1}): 3309, 3156, 2196, 1718, 1675, 1571, 1470, 1395, 1339, 1104. ^{1}H NMR (400 MHz, DMSO-d_6) δ (ppm): 6.77 (d, 1H, Ar–H, J = 8.0 Hz), 6.89 (t, 1H, Ar–H, J = 8.0 Hz), 7.13 (t, 1H, Ar–H, J = 2.0 Hz), 7.15 (d, 1H, Ar–H, J = 8.0 Hz), 7.33 (s, 2H, NH_2), 10.48 (s, 1H, NH), 12.15 (s, 1H, NH), 13.85 (s, 1H, NH).

7′-Amino-2,2′,4′-trioxo-1′,2′,3′,4′-tetrahydrospiro[indoline-3,5′-pyrano[2,3-d]pyrimidine]-6′-carbonitrile. White solid, mp 275–277 °C, lit. [28] (mp 274–276 °C). IR (KBr) ν(cm^{-1}): 3353, 3304, 3145, 2829, 2203, 1723, 1673, 1395, 1616, 1531, 1468, 1337, 1111. ^{1}H NMR (400 MHz, DMSO-d_6) δ (ppm): 6.77 (d, 1H, Ar–H, J = 8.0 Hz), 6.89 (t, 1H, Ar–H, J = 6.0 Hz), 7.12 (d, 1H, Ar–H, J = 8.0 Hz), 7.15 (d, 1H, Ar–H, J = 4.0 Hz), 7.37 (s, 2H, NH_2), 10.47 (s, 1H, NH), 11.12 (s, 1H, NH), 12.30 (s, 1H, NH).

7′-Amino-5-chloro-2,4′-dioxo-2′-thioxo-1′,2′,3′,4′-tetrahydro spiro[indoline-3,5′-pyrano[2,3-d]pyrimidine]-6′-carbonitrile. White solid, mp 228–230 °C, lit. [28] (mp 224–226 °C). IR (KBr) ν(cm^{-1}): 3358, 3278, 3150, 2849, 2196, 1679, 1570, 1476, 1340, 1172, 1110, 1066. ^{1}H NMR (400 MHz, DMSO-d_6) δ (ppm): 6.79 (d, 1H, Ar–H, J = 8.0 Hz), 7.19–7.22 (dd, 1H, Ar–H, J = 12.0 Hz, J = 4.0

Open Access Article. Published on 10 May 2021. Downloaded on 1/20/2026 11:24:10 AM.
This article is licensed under a Creative Commons Attribution-NonCommercial 3.0 Unported Licence.

Hz), 7.37 (d, 1H, Ar–H, J = 4.0 Hz), 7.47 (s, 2H, NH_2), 10.65 (s, 1H, NH), 12.43 (s, 1H, NH), 13.86 (s, 1H, NH).

7′-Amino-5-chloro-2,2′,4′-trioxo-1′,2′,3′,4′-tetrahydrospiro [indoline-3,5′-pyrano[2,3-d]pyrimidine]-6′-carbonitrile. White solid, mp 242–245 °C, lit. [29] (mp 250–258 °C). IR (KBr) ν(cm^{-1}): 3296, 3163, 2821, 2200, 1693, 1644, 1537, 1401, 1336, 1121, 999. ^{1}H NMR (400 MHz, DMSO-d_6) δ (ppm): 6.78 (d, 1H, Ar–H, J = 8.0 Hz), 7.18–7.21 (dd, 1H, Ar–H, J = 12.0 Hz, J = 4.0 Hz), 7.31 (d, 1H, Ar–H, J = 8.0 Hz), 7.43 (s, 2H, NH_2), 10.60 (s, 1H, NH), 11.12 (s, 1H, NH), 12.32 (s, 1H, NH).

2-Amino-5′-chloro-2′,5-dioxo-5H-spiro[indeno[1,2-b]pyran-4,3′-indoline]-3-carbonitrile. Yellow solid, mp 219–222 °C. IR (KBr) ν(cm^{-1}): 3316, 3241, 3199, 2196, 1738, 1667, 1600, 1472, 1334, 1209, 923. ^{1}H NMR (400 MHz, DMSO-d_6) δ (ppm): 6.89 (d, 1H, Ar–H, J = 8 Hz), 7.26 (d, 1H, Ar–H, J = 4.0 Hz), 7.30 (d, 1H, Ar–H, J = 8.0 Hz), 7.37 (d, 1H, Ar–H, J = 8.0 Hz), 7.43 (d, 1H, Ar–H, J = 8.0 Hz), 7.45 (d, 1H, Ar–H, J = 8.0 Hz), 7.56 (t, 1H, Ar–H, J = 6.0 Hz), 7.78 (s, 2H, NH_2), 10.83 (s, 1H, NH). ^{13}C NMR (100 MHz, DMSO-d_6) δ (ppm): 46.55, 56.96, 106.47, 112.36, 117.68, 118.87, 122.20, 124.98, 126.61, 129.06, 130.51, 131.33, 133.62, 134.37, 135.16, 140.70, 160.55, 167.83, 176.25, 189.35.

Ethyl-2-amino-5′-chloro-7,7-dimethyl-2′,5-dioxo-5,6,7,8-tetrahydrospiro[chromene-4,3′-indoline]-3-carboxylate. White solid, mp 278–281 °C, lit. [30] (mp 275–278 °C). IR (KBr) ν(cm^{-1}): 3384, 3276, 2958, 1725, 1687, 1650, 1514, 1477, 1349, 1294, 1052. ^{1}H NMR (400 MHz, DMSO-d_6) δ (ppm): 0.81 (t, 3H, CH_3, J = 6.0 Hz), 0.95 (s, 3H, CH_3), 0.99 (s, 3H, CH_3), 2.04–2.15 (q, 2H, CH_2, J = 16.0 Hz), 2.50 (t, 2H, CH_2, J = 2.0 Hz), 3.67–3.70 (m, 2H, CH_2), 6.67 (d, 1H, Ar–H, J = 8.0 Hz), 6.89 (d, 1H, Ar–H, J = 4.0 Hz), 7.07–7.09 (dd, 1H, Ar–H, J = 8.0 Hz, J = 4 Hz), 7.93 (s, 2H, NH_2), 10.31 (s, 1H, NH).

Ethyl-2-amino-7,7-dimethyl-2′,5-dioxo-5,6,7,8-tetrahydrospiro [chromene-4,3′-indoline]-3-carboxylate. White solid, mp 252–254 °C, lit. [30] (mp 256–258 °C). IR (KBr) ν(cm^{-1}): 3369, 3178, 2958, 1715, 1688, 1613, 1525, 1473, 1316, 1259. ^{1}H NMR (400 MHz, DMSO-d_6) δ (ppm): 0.78 (t, 3H, CH_3, J = 6.0 Hz), 0.93 (s, 3H, CH_3), 0.97 (s, 3H, CH_3), 2.00 (d, 1H, CH, J = 16.0 Hz), 2.14 (d, 1H, CH, J = 16.0 Hz), 2.47 (d, 1H, CH, J = 16.0 Hz), 2.57 (d, 1H, CH, J = 16.0 Hz), 3.68–3.70 (m, 2H, CH_2), 6.66 (d, 1H, Ar–H, J = 8.0 Hz), 6.75 (t, 1H, Ar–H, J = 6.0 Hz), 6.82 (d, 1H, Ar–H, J = 8.0 Hz), 7.03 (t, 1H, Ar–H, J = 8.0 Hz), 7.85 (s, 2H, NH_2), 10.13 (s, 1H, NH).

2-Amino-5′-chloro-7,7-dimethyl-2′,5-dioxo-5,6,7,8-tetrahydro spiro[chromene-4,3′-indoline]-3-carbonitrile. White solid, mp 292–294 °C, lit. [30] (mp > 300 °C). IR (KBr) ν(cm^{-1}): 3286, 3154, 2958, 2192, 1726, 1652, 1602, 1475, 1350, 1222, 1056. ^{1}H NMR (400 MHz, DMSO-d_6) δ (ppm): 1.01 (s, 6H, $2CH_3$), 2.14 (s, 2H, CH_2), 2.54 (d, 2H, CH_2, J = 12.0 Hz), 6.79 (d, 1H, Ar–H, J = 8.0 Hz), 7.09 (d, 1H, Ar–H, J = 4.0 Hz), 7.17–7.19 (dd, 1H, Ar–H, J = 8.0 Hz, J = 4.0 Hz), 7.33 (s, 2H, NH_2), 10.54 (s, 1H, NH).

3′-Acetyl-6′-amino-5-chloro-2′-methyl-2-oxo-spiro[indoline-3,4′-pyran]-5′-carbonitrile. White solid, mp 280–282 °C. IR (KBr) ν(cm^{-1}): 3356, 3237, 2192, 1705, 1653, 1592, 1479, 1298, 1214, 1054. ^{1}H NMR (400 MHz, DMSO-d_6) δ (ppm): 2.22 (s, 3H, CH_3), 2.38 (s, 3H, CH_3), 6.77 (d, 1H, Ar–H, J = 8.0 Hz), 7.10 (d, 1H, Ar–

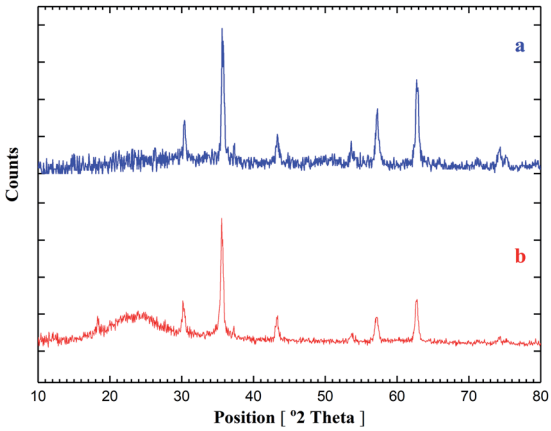

Fig. 1 XRD spectrum of (a) $CoFe_2O_4$, (b) $CoFe_2O_4$@SiO_2-guanidine.

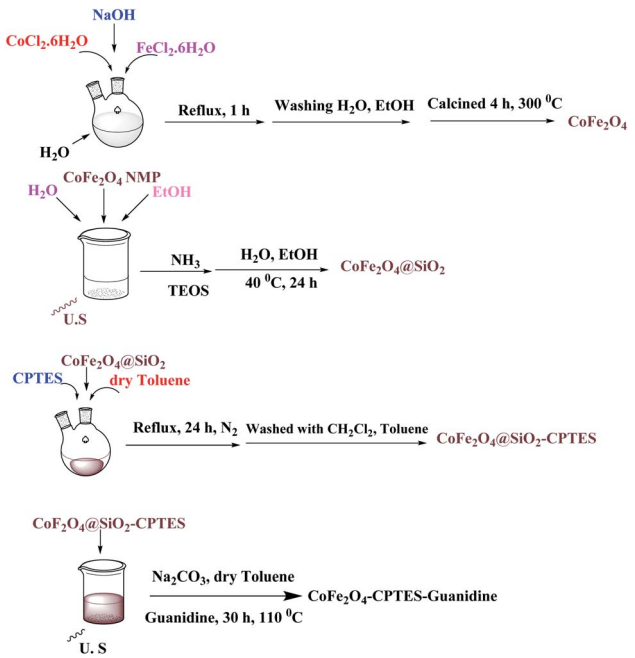

Scheme 1 Synthesis of the $CoFe_2O_4$@SiO_2-guanidine catalyst.

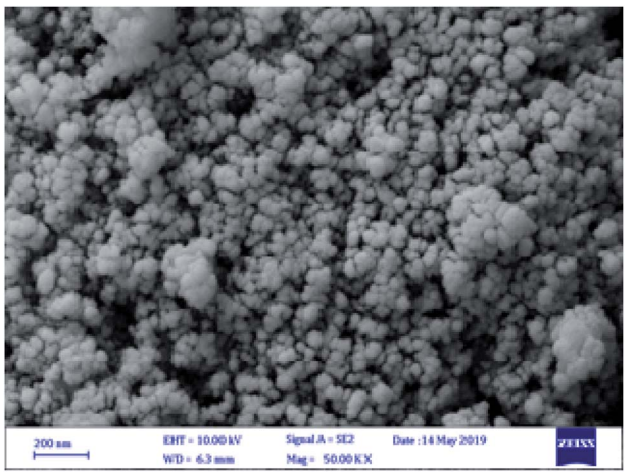

Fig. 2 SEM images of $CoFe_2O_4$@SiO_2-guanidine.

© 2021 The Author(s). Published by the Royal Society of Chemistry

Open Access Article. Published on 10 May 2021. Downloaded on 1/20/2026 11:24:10 AM.
This article is licensed under a Creative Commons Attribution-NonCommercial 3.0 Unported Licence.

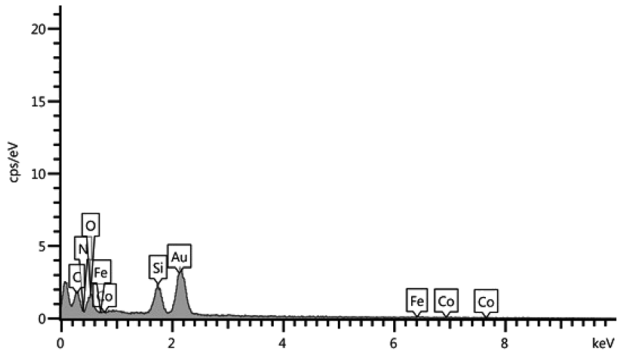

Fig. 3 The EDX pattern of the $CoFe_2O_4$@SiO_2-guanidine.

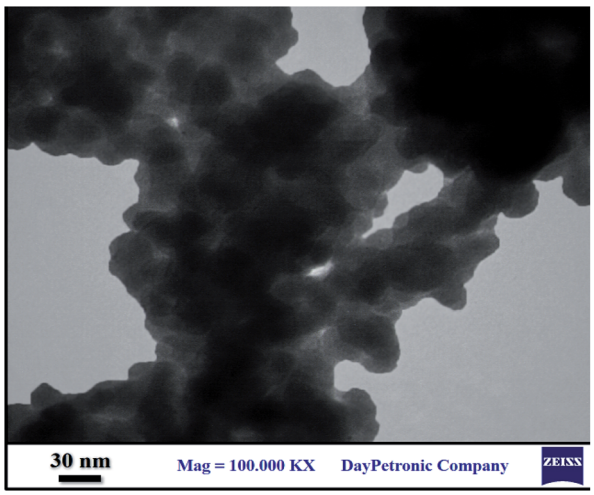

Fig. 4 The TEM image of the $CoFe_2O_4$@SiO_2-guanidine.

H, $J = 4.0$ Hz), 7.16 (d, 1H, Ar–H, $J = 4.0$ Hz), 7.20 (s, 2H, NH_2), 10.49 (s, 1H, NH). ^{13}C NMR (100 MHz, DMSO-d_6) δ (ppm): 19.80, 31.53, 56.13, 110.67, 114.41, 117.36, 123.19, 125.61, 128.15, 136.69, 140.88, 158.05, 159.01, 178.33, 197.03.

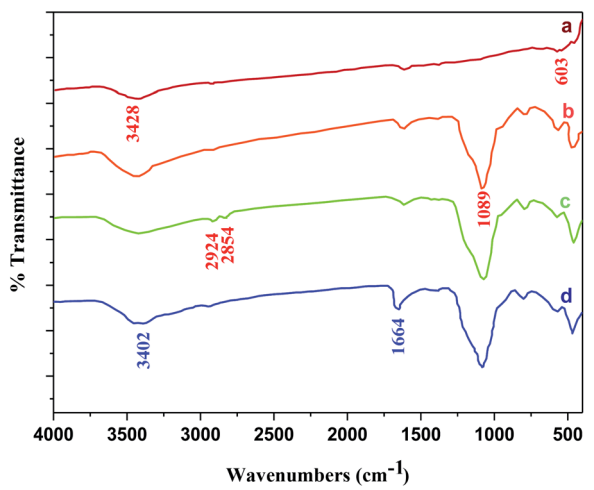

Fig. 5 FT-IR spectra of (a) $CoFe_2O_4$ nanoparticles, (b) $CoFe_2O_4$@SiO_2, (c) $CoFe_2O_4$@SiO_2-CPTES, (d) $CoFe_2O_4$@SiO_2-guanidine.

2-Amino-7,7-dimethyl-2′,5-dioxo-5,6,7,8-tetrahydrospiro [chromene-4,3′-indoline]-3-carbonitrile. White solid, mp 288–290 °C, lit. [30] (mp 290–292 °C). IR (KBr) ν(cm^{-1}): 3375, 3312, 3142, 2960, 2192, 1722, 1655, 1604, 1469, 1349, 1220, 1054. ^{1}H NMR (400 MHz, DMSO-d_6) δ (ppm): 0.99 (s, 3H, CH_3), 1.02 (s, 3H, CH_3), 2.06–2.18 (q, 2H, CH_2, $J = 16$ Hz), 2.54 (d, 2H, CH_2, $J = 4.0$ Hz), 6.77 (d, 1H, Ar–H, $J = 8.0$ Hz), 6.88 (t, 1H, Ar–H, $J = 8.0$ Hz), 6.97 (d, 1H, Ar–H, $J = 8.0$ Hz), 7.13 (t, 1H, Ar–H, $J = 8.0$ Hz), 7.23 (s, 2H, NH_2), 10.39 (s, 1H, NH).

3′-Acetyl-6′-amino-2′-methyl-2-oxo-spiro[indoline-3,4′-pyran]-5′-carbonitrile. White solid, mp 240–243 °C, lit. [31] (mp 243–245 °C). IR (KBr) ν(cm^{-1}): 3378, 3346, 3120, 2188, 1709, 1680, 1653, 1467, 1296, 1211. ^{1}H NMR (400 MHz, DMSO-d_6) δ (ppm): 2.13 (s, 3H, CH_3), 2.28 (s, 3H, CH_3), 6.76 (d, 1H, Ar–H, $J = 8.0$ Hz), 6.90 (t, 1H, Ar–H, $J = 8.0$ Hz), 7.02 (d, 1H, Ar–H, $J = 8.0$ Hz), 7.12 (s, 2H, NH_2), 7.15 (d, 1H, Ar–H, $J = 8.0$ Hz), 10.38 (s, 1H, NH).

3. Results and discussion

3.1. Preparation and characterization of catalyst

To prepare the catalyst, we have chosen a mixture of $CoCl_2 \cdot 6H_2O$, $FeCl_3 \cdot 6H_2O$ and NaOH dissolved in deionized water

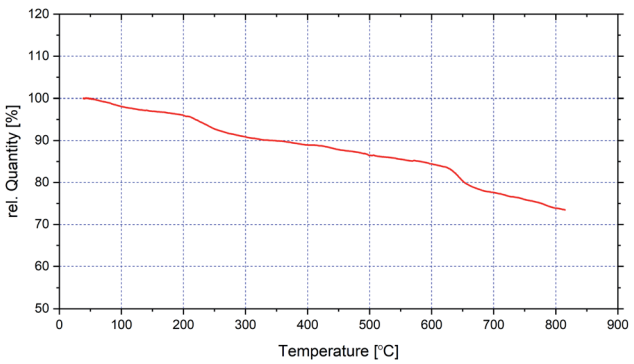

Fig. 6 TG analysis of $CoFe_2O_4$@SiO_2-guanidine.

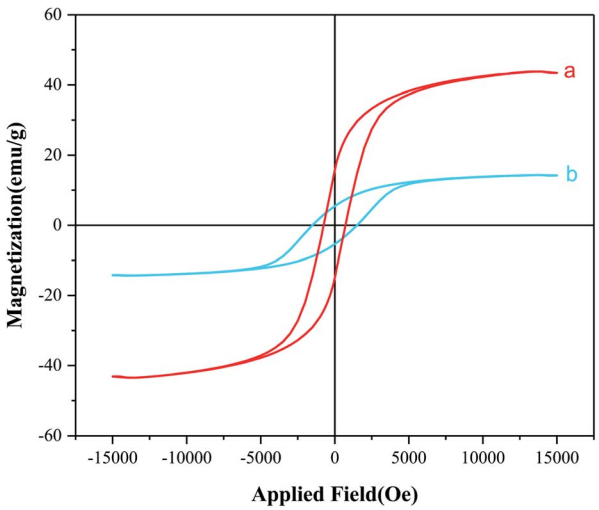

Fig. 7 Magnetization curves for (a) $CoFe_2O_4$ and (b) $CoFe_2O_4$@SiO_2-guanidine.

Open Access Article. Published on 10 May 2021. Downloaded on 1/20/2026 11:24:10 AM.
This article is licensed under a Creative Commons Attribution-NonCommercial 3.0 Unported Licence.

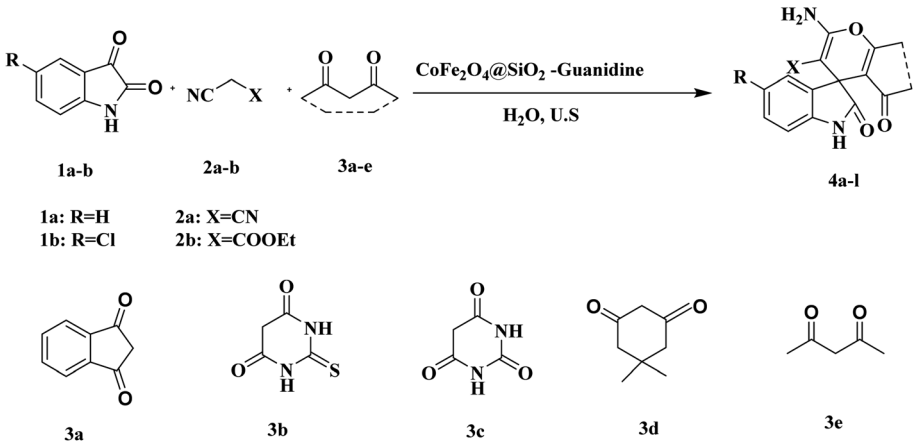

Scheme 2 The preparation of spirooxindole derivatives using nanocomposites as catalyst.

under reflux condition according to the procedure reported in the literature.[18] In the next step, the nanomagnetic was coated with silica. Then, the resulting silica-coated $CoFe_2O_4$ nanoparticles were allowed to react under vigorous stirring with an appropriate concentration of 3-chloropropyltriethoxysilane.[25,26] Finally, the reaction of $CoFe_2O_4$@SiO_2 carried out with guanidine in toluene under reflux condition for 30 h to give amino-functionalized silica-coated nanomagnetic ($CoFe_2O_4$@SiO_2-guanidine). The synthetic path for preparation of the catalyst is shown in Scheme 1. In order to characterize the catalyst structure, the synthesized nanocatalyst was analysed using XRD, SEM, EDX, TEM, FT-IR, TGA and VSM techniques.

The structure of the magnetic nanocatalyst was characterized by XRD as shown in Fig. 1. There are six diffraction peaks at 2θ about 30.26, 35.61, 43.24, 53.73, 57.16 and 62.72 corresponding to the (220), (311), (400), (422), (511) and (440) planes in the $CoFe_2O_4$ which is correspond to the standard pattern. As shown in Fig. 1, the positions of all peaks in the XRD pattern of $CoFe_2O_4$@SiO_2-guanidine were according to standard XRD pattern of $CoFe_2O_4$.

The morphology of the $CoFe_2O_4$@SiO_2-guanidine magnetic nanocomposite was determined by SEM. The average size of nanoparticles on the support determined from Fig. 2 was about 54 nm.

The EDX pattern shown in Fig. 3 confirms the signals for carbon, iron, cobalt, oxygen, nitrogen and silicon elements. The results of EDX, XRD and SEM for $CoFe_2O_4$@SiO_2-guanidine nanocomposite confirm that nanoparticles were exactly fabricated on the surface.

The TEM image of the nanocomposite was shown in Fig. 4. This image displays the formation of $CoFe_2O_4$@SiO_2-guanidine nanostructure that contains core–shell nature.

Furthermore, the Fig. 5a–d shows the FT-IR spectra of $CoFe_2O_4$ MNPs, $CoFe_2O_4$@SiO_2, $CoFe_2O_4$@SiO_2-CPTES and $CoFe_2O_4$@SiO_2-guanidine, respectively. The FT-IR spectrum of $CoFe_2O_4$ MNPs shows peaks characteristic of Co–O at 603 cm^{-1} and the broad band at 3428 cm^{-1} is due to the O–H of adsorbed

Table 1 Effect of different amounts of the catalyst on the reaction [a]

Entry	Amount of catalyst (mg)	Time (min)	Yield[b] (%)
1	No catalyst	10	—
2	2	10	20
3	4	10	40
4	6	10	65
5	8	10	70
6	9	10	70

[a] Reaction condition: isatin (1 mmol), malononitrile (1 mmol), dimedone (1 mmol) under ultrasonic irradiation and water as a solvent. [b] Isolated yield.

Table 2 Optimization of ultrasonic power by using $CoFe_2O_4$@SiO_2-CPTES-guanidine in water[a]

Entry	Power (W)	Time (min)	Yield (%)
1	30	10	70
2	35	10	84
3	40	10	90
4	45	10	90

[a] Reaction condition: isatin (1 mmol), malononitrile (1 mmol), dimedone (1 mmol) under ultrasonic irradiation and water as a solvent.

Table 3 Optimization of solvents in the presence of $CoFe_2O_4$@SiO_2-guanidine (8 mg) under ultrasonic irradiation (40 W)[a]

Entry	Solvent	Time (min)	Yield[b] (%)
1	EtOH	10	68
2	Water	10	90
3	DMF	10	50
4	Chloroform	10	20
5	Toluene	10	15

[a] Reaction condition: isatin (1 mmol), malononitrile (1 mmol), dimedone (1 mmol) and $CoFe_2O_4$@SiO_2-guanidine (8 mg) under ultrasound irradiation (40 W), at sonicated time. [b] Isolated yields.

© 2021 The Author(s). Published by the Royal Society of Chemistry

Open Access Article. Published on 10 May 2021. Downloaded on 1/20/2026 11:24:10 AM.
This article is licensed under a Creative Commons Attribution-NonCommercial 3.0 Unported Licence.

Table 4 The preparation of spirooxindole derivatives using $CoFe_2O_4$@SiO_2-guanidine as catalyst at green conditions[a]

Entry	Isatin	Nitril	Carbonyl compound	Product	Time (min)	Yield[b] (%)
1	**1a**	**2a**	**3a**	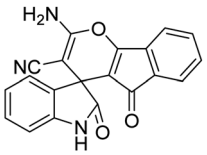	15	94
2	**1a**	**2a**	**3b**	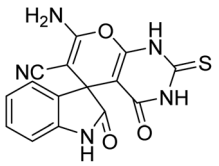	10	92
3	**1a**	**2a**	**3c**	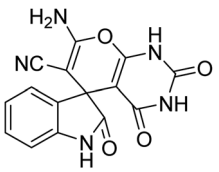	8	92
4	**1b**	**2a**	**3b**	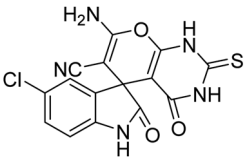	10	91
5	**1b**	**2a**	**3c**	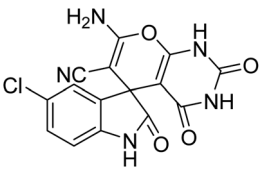	10	93
6	**1b**	**2a**	**3a**	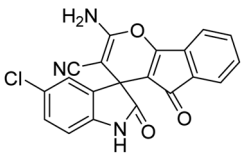	12	92
7	**1b**	**2b**	**3d**	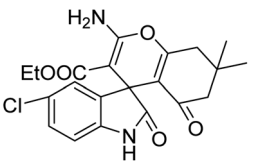	15	88
8	**1a**	**2b**	**3d**	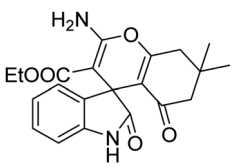	15	90
9	**1b**	**2a**	**3d**	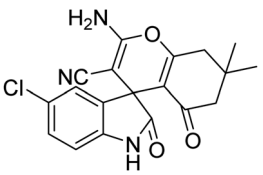	10	87

© 2021 The Author(s). Published by the Royal Society of Chemistry

Open Access Article. Published on 10 May 2021. Downloaded on 1/20/2026 11:24:10 AM.
This article is licensed under a Creative Commons Attribution-NonCommercial 3.0 Unported Licence.

Table 4 (*Contd.*)

Entry	Isatin	Nitril	Carbonyl compound	Product	Time (min)	Yield[b] (%)
10	**1b**	**2a**	**3e**	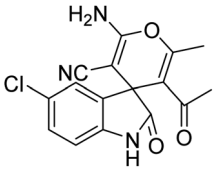	10	92
11	**1a**	**2a**	**3d**	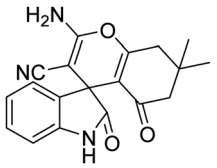	10	90
12	**1a**	**2a**	**3e**	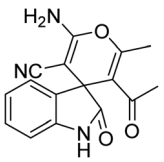	8	92

[a] Reaction condition: isatin/5-chloroisatin (1 mmol), malononitrile/cyanoacetic esters (1 mmol), 1,3-dicarbonyl compounds and $CoFe_2O_4$@SiO_2-guanidine (8 mg) under ultrasound irradiation (40 W), water as a solvent condition. [b] Isolated yields.

water molecule and silica surface (Fig. 5a). Fig. 1b shows the FT-IR spectrum of $CoFe_2O_4$@SiO_2 MNPs. The band at 1089 cm^{-1} is attributed to the vibration of Si–O–Si bonds (Fig. 5b). Fig. 5c shows the FT-IR spectrum of the $CoFe_2O_4$@SiO_2-CPTES. The FT-IR spectrum shows two peaks at 2924 and 2854 cm^{-1} which are related to C–H stretching vibrations. In comparison to $CoFe_2O_4$@SiO_2-CPTES, the presence of new bands in $CoFe_2O_4$@SiO_2-guanidine is observed and the guanidine is recognized by the presence of stretching vibrations of N–H bonds at 3402 cm^{-1}. The stretching vibration of C=N bonds at 1664 cm^{-1} are indicated (Fig. 5d).

In Fig. 6, the TG analysis of $CoFe_2O_4$@SiO_2-guanidine are displayed. The primary small weight loss about 5% below 200 °C which corresponds to the removal of physically adsorbed solvent and surface hydroxyl groups. The weight loss observed about 15% between 200–800 °C in TGA curve of $CoFe_2O_4$@SiO_2-guanidine is mainly related to the decomposition of supported organic components on the nanoparticles (Fig. 6).

Magnetic properties of $CoFe_2O_4$ nanoparticles, $CoFe_2O_4$@SiO_2-guanidine were investigated by VSM technique at room temperature. As shown in Fig. 7, MNPs to 15 emu g^{-1} in the final $CoFe_2O_4$@SiO_2-guanidine catalyst. These consequences show that the magnetization property reduces *via* coating and functionalization surface of the $CoFe_2O_4$ nanoparticles. But the advantage of the nanocomposite is that can be easily separated by an external magnet from the mixture reaction after the catalytic reaction.

Finally, the prepared $CoFe_2O_4$@SiO_2-guanidine was used as heterogeneous catalyst in the reaction of isatin or 5-chloroisatin, malononitrile or cyanoacetic ester and 1,3-dicarbonyl compounds in 1 : 1 : 1 mole ratio under ultrasonic irradiation and water as a solvent (Scheme 2).

To optimize the reaction conditions in amount of catalyst, condensation of isatin (1 mmol), malononitrile (1 mmol), dimedone (1 mmol) was selected as a model reaction and studied under different conditions.

In order to obtain the optimal amount of the catalyst, the reaction was carried out in the presence of different amounts of catalyst under ultrasonic irradiation and water as a solvent (Table 1).

Table 5 Comparison of the present work with previously reported works for synthesis of spirooxindoles

Entry	Catalyst	Condition	Time (min)	Yield (%)	Ref.
1	Fe_3O_4@SiO_2-imid-PMA	Reflux, H_2O	90	93	32
2	SBA-Pr-NH_2	Reflux, H_2O	5	91	33
3	ZnS NP	U. S, H_2O	11	95	34
4	MgO NP	Thermal, H_2O	120	95	35
5	Cs_xH_{3-X} $PW_{12}O_{40}$NP	Thermal, CH_3CN	90	88	36
6	$CoFe_2O_4$@SiO_2-guanidine	U. S, H_2O	10	90	This work

© 2021 The Author(s). Published by the Royal Society of Chemistry

Open Access Article. Published on 10 May 2021. Downloaded on 1/20/2026 11:24:10 AM.
This article is licensed under a Creative Commons Attribution-NonCommercial 3.0 Unported Licence.

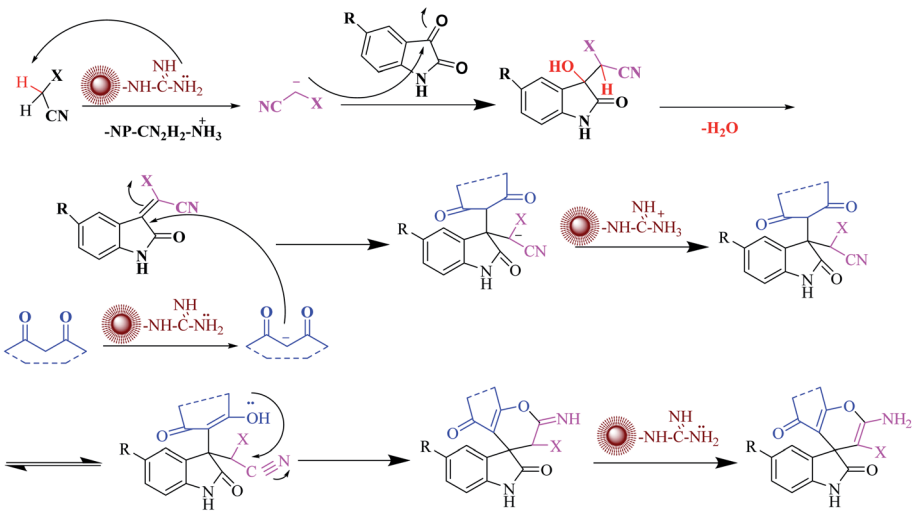

Scheme 3 Proposed reaction mechanism for spirooxindole derivatives by $CoFe_2O_4$@SiO_2-guanidine nanocomposite as a catalyst.

As can be seen in Table 1, the reaction was efficiently performed using 8 mg of the catalyst under ultrasonic irradiation and water as a solvent and the desired product was obtained in high yield within a short reaction time (Table 1, entry 5).

After the optimization of the catalyst amount, the reaction was carried out in water under ultrasonic irradiation at different powers (Table 2). In the same way, the highest yield of product was resulted from the reaction run under ultrasonic irradiation with a power of 40 W (Table 2, entry 3).

In continuation, the reaction of isatin (1 mmol), malononitrile (1 mmol), dimedone (1 mmol) and $CoFe_2O_4$@SiO_2-guanidine (8 mg) as catalyst and power of 40 W was carried out in various solvents (Table 3). The best results were obtained using water as a solvent (Table 3, entry 2).

After optimization of the catalyst amount, ultrasonic power and optimization of solvents, synthesis of spirooxindole derivatives were carried out. The corresponding results are depicted in Table 4.

The present work was compared with the previously reported works for synthesis of spirooxindoles and the results are shown in Table 5. It was found that the present work was the better than the other works on the basis of reaction times, product yields and used catalyst amounts for the reactions (Table 5, entry 6 *vs.* entries 1–5).

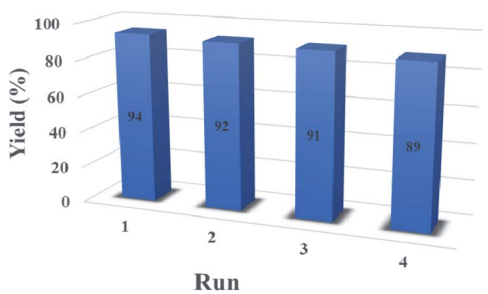

Fig. 8 The reusability of the $CoFe_2O_4$@SiO_2-guanidine catalyst.

In a plausible mechanism, at first, malononitrile is activated by catalyst and attacks to the carbonyl group of isatin and removes of H_2O. Then, in second step, 1,3-dicarbonyl compounds is activated by catalyst and attacks to the α carbon atom of isatin. Then a tautomer is performed and the hydroxyl group attack on the carbon of nitrile and the final product is produced (Scheme 3).

3.2. Catalyst reusability

As shown in Fig. 8, it was investigated the reusability of $CoFe_2O_4$@SiO_2-guanidine as heterogeneous catalyst for the reaction of isatin, malononitrile, indandion as a model reaction. After the completion of the reaction, the catalyst was separated from the reaction mixture using an external magnet and the residual catalyst was washed with ethyl acetate and dried in an oven at 50 °C. The recycled catalyst could be reused for three times without considerable loss of its catalytic activity.

4. Conclusion

In summary, this paper proposed a new protocol for the synthesis of spirooxindole derivatives in the presence of $CoFe_2O_4$@SiO_2-guanidine nanocomposites (core–shell) as a nanocatalyst in water as a solvent under ultrasonic irradiation. The main advantages of this present procedure are the easy recovery of catalyst, non-toxic, small amount of used catalyst and given products with high yields and short reaction times.

Conflicts of interest

There are no conflicts to declare.

Acknowledgements

The authors are grateful to University of Kashan for supporting this work by Grant No. 159148/85.

Open Access Article. Published on 10 May 2021. Downloaded on 1/20/2026 11:24:10 AM.
This article is licensed under a Creative Commons Attribution-NonCommercial 3.0 Unported Licence.

References

1 J. S. Bindra, *The Alkaloides: Chemistry and Physiology*, 1973, vol. 14, pp. 83–121.
2 C. V. Galliford and K. A. Scheidt, *Angew. Chem., Int. Ed.*, 2007, **46**, 8748.
3 P. B. Alper, C. Meyers, A. Lerehner, D. R. Siegel and E. M. Carreira, *Angew. Chem., Int. Ed.*, 1999, **38**, 3186.
4 W. Kemnitzer, J. Drewe, S. Jiang, H. Zhang, Y. Wang, J. Zhao, S. Jia, J. Herich, D. Labreque, R. Storer, K. Meerovitch, D. Bouffard, R. Rej, R. Denis, C. Blais, S. Lamothe, G. Attardo, H. Gourdeau, B. Tseng, S. Kasilbhatla and S. X. Cai, *J. Med. Chem.*, 2004, **47**, 6299.
5 A. H. Abdel-Rahman, E. M. Keshk, M. A. Hanna and Sh. M. El-Bady, *Bioorg. Med. Chem.*, 2004, **12**, 2483.
6 S. Riyaz, A. Naidu and P. K. Dubey, *Lett. Org. Chem.*, 2012, **9**, 101–105.
7 M. Kidwai, A. Jahan and N. K. Mishra, *Appl. Catal., A*, 2012, 425–426.
8 G. Shanthi, G. Subbulakshmi and P. T. Perumal, *Tetrahedron*, 2007, **63**, 2057–2063.
9 L. M. Wang, N. Jiao, J. Qiu, J. J. Yu, J. Q. Liu, F. L. Guo and Y. Liu, *Tetrahedron*, 2010, **66**, 339–343.
10 G. S. Hari and Y. R. Lee, *Synthesis*, 2010, **3**, 453–464.
11 F. Kiani and H. Naeimi, *Ultrason. Sonochem.*, 2018, **48**, 267–274.
12 H. Naeimi and R. Shaabani, *Ultrason. Sonochem.*, 2017, **34**, 246–254.
13 H. Xu, B. W. Zeiger and K. S. Suslick, *Chem. Soc. Rev.*, 2013, **42**, 2555–2567.
14 T. J. Mason, *Ultrason. Sonochem.*, 2003, **10**, 175–179.
15 C. L. Ni, X. H. Song, H. Yan, X. Q. Song and R. G. Zhong, *Ultrason. Sonochem.*, 2010, **17**, 367–369.
16 K. S. Suslick, S. B. Choe, A. A. Cichowlas and M. W. Grinstaff, *Nature*, 1991, **353**, 414.
17 S. J. Oldenberg, R. D. Averitt, S. L. Westcott and N. Halas, *J. Phys. Chem. Lett.*, 1998, **288**, 243.
18 M. Shaker and D. Elhamifar, *New J. Chem.*, 2020, **44**, 3445–3454.
19 M. Norouzi and D. Elhamifar, *Composites, Part B*, 2019, **176**, 107308.
20 M. Neysi, A. Zarnegaryan and D. Elhamifar, *New J. Chem.*, 2019, **43**, 12283–12291.
21 M. Norouzi, D. Elhamifar and R. Mirbagheri, *Microporous Mesoporous Mater.*, 2019, **278**, 251–256.
22 R. Mirbagheri and D. Elhamifar, *J. Alloys Compd.*, 2019, **790**, 783–791.
23 Z. Ramazani, D. Elhamifar, M. Norouzi and R. Mirbagheri, *Composites, Part B*, 2019, **164**, 10–17.
24 S. Abaeezadeh, D. Elhamifar, M. Norouzi and M. Shaker, *Appl. Organomet. Chem.*, 2019, **33**, e4862.
25 P. H. Li, B. L. Li, Z. M. An, L. P. Mo, Z. S. Cui and Z. H. Zhang, *Adv. Synth. Catal.*, 2013, **355**, 2952–2959.
26 L. Heidari and L. Shiri, *Appl. Organomet. Chem.*, 2019, **33**, 4636.
27 R. Jamatia, A. Gupta and A. K. Pal, *RSC Adv.*, 2016, **6**, 20994–21000.
28 D. R. Chandam, A. G. Mulik, D. R. Patil and M. B. Deshmukh, *Res. Chem. Intermed.*, 2016, **42**, 1411–1423.
29 A. Khalafi-Nezhad, E. Shaikhi-Shahidzadeh, S. Sarikhani and F. Panahi, *J. Mol. Catal. A: Chem.*, 2013, **379**, 1–8.
30 Y. Li, H. Chen, C. Shi, D. Shi and S. Ji, *J. Comb. Chem.*, 2010, **12**, 231–237.
31 F. Mohamadpour, M. T. Maghsoodlou, M. Lashkari, R. Heydari and N. Hazeri, *Org. Prep. Proced. Int.*, 2019, **51**, 456–476.
32 M. Esmaeilpour, J. Javidi and M. Divar, *J. Magn. Magn Mater.*, 2017, **423**, 232–240.
33 G. M. Ziarani, A. Badiei, S. Mousavi, N. Lashgari and A. Shahbazi, *Chin. J. Catal.*, 2012, **33**, 1832–1839.
34 A. Dandia, V. Parewa, A. Kumar Jaina and K. S. Rathore, *Green Chem.*, 2011, **13**, 2135.
35 B. Karmakar, A. Nayak and J. Banerji, *Tetrahedron Lett.*, 2012, **53**, 5004–5007.
36 S. Pradhan and B. G. Mishra, *J. Mol. Catal.*, 2018, **446**, 58–71.

© 2021 The Author(s). Published by the Royal Society of Chemistry